

Precise calculation of the optical constants of self-standing nanoporous silicon layers

Rehab Ramadan (✉ rehabramadan@mu.edu.eg)

Minia University

Raúl J. Martín-Palma

Universidad Autónoma de Madrid

Research Article

Keywords: Porous silicon, optical constants, energy bandgap, computational matrix method

Posted Date: November 16th, 2022

DOI: <https://doi.org/10.21203/rs.3.rs-2237632/v1>

License: © ⓘ This work is licensed under a Creative Commons Attribution 4.0 International License.

[Read Full License](#)

Additional Declarations: No competing interests reported.

Version of Record: A version of this preprint was published at Silicon on February 25th, 2023. See the published version at <https://doi.org/10.1007/s12633-023-02358-x>.

Abstract

The precise knowledge of the values of the optical constants (index of refraction, n , and extinction coefficient, k) for nanostructured porous silicon (nanoPS) is a necessary condition to predict the behavior of any optical and photonic devices based on this material. With this objective in mind, a simulation computational program based on the matrix method was used to determine the values of the optical constants in the visible range of self-standing nanoPS films from their experimental reflectance and transmittance spectra. Furthermore, the spectral absorption coefficient (α) was determined from the spectral k values, which motivated to the determination of the values and type of bandgap (direct or indirect) for different porosities

1. Introduction

Thin film optical coatings are used to modify the response of photonic devices. The index of refraction of the single thin films, number of layers and their thickness are the main parameters that affect the response of multilayer optical coatings. The optical coatings might be in bulk thin film form or nanostructured layer grown by different physical and chemical methods [1–3].

Within this context, the precise determination of the optical properties of thin films is essential for the subsequent development of optical devices. Three key parameters are the index of refraction (n), extinction coefficient (k), and energy bandgap (E_g). The optical constants of thin films can be determined from optical measurements, i.e., transmission and reflection [4] or by ellipsometry [5]. For the design of optical coatings with the required properties it is essential a great accuracy in the determination of the optical constants since a minimum variation of these values would lead to a deterioration of the behavior of the whole coating. The degradation of the optical performance would increase with increasing number of layers.

Nanostructured porous silicon (nanoPS) is one of the common materials applied in a variety of photonic devices due to the facile management of its optical response depending on its morphology [6–8]. NanoPS can be described as a mixture of air, amorphous silicon, silicon nanocrystals and silicon dioxide [9, 10], strongly depend on the structure of the fabricated layer [11]. The structure of this material can be widely adjusted through the fabrication parameters. NanoPS layers can be fabricated by different methods. For instance, by electrochemical etching [10], electroless method [12] and by photolithography method [13]. The optical property of such material has a main function in the morphology and thickness of the nanoPS layers.

In the current work, fabrication of self-standing nanoPS layers with different porosities was carried out by electrochemical etching process followed by electropolishing. Furthermore, an accurate determination of the values of the optical constants of nanostructured self-standing porous silicon layers at different porosities, which would allow exploiting the unique optical properties of this material for the development

of such devices as light emitting diodes, filtered photodetectors, optical sensors, and photovoltaic solar cells.

2. Theoretical And Experimental Techniques

2.1. THEORETICAL MODEL

A computational simulation method based on a matrix method was used to obtain a precise determination of the optical constants of self-standing nanoPS layers. The software is based on spectral reflectance and transmittance data. In this case, the materials under study is described as a plane-parallel layer of infinite extent, characterized by an index of refraction n and an extinction coefficient k [14]. Accordingly, each interface and homogeneous layer in a multilayer coating is described by its appropriate matrix. The values of the optical constants are a function of the film thickness and index of refraction [15]. Therefore, the resultant matrix, M_R of a series of parallel layers is given by $M_R = M_1 \times M_2 \times \dots$, so the final result is expressed in terms of the product of a set of 2×2 matrices [16]. The accuracy of the simulated results depends on some considerations to be able to apply this formalism, which is addressed in reference [17].

2.2. EXPERIMENTAL

Self- standing membranes of nanoPS were fabricated by the electrochemical etch of p-type silicon wafer of $< 100 >$ orientation and resistivity (0.01–0.02 $\Omega \cdot \text{cm}$) followed by electropolishing process. The etching process was carried out at room temperature in a 1:2 mixture of HF (48%): ethanol (98%). The experimental setup of the electrochemical etching system has been described in a previous study [15]. To detach the nanoPS layer from the underlying silicon wafer, an etching current density of 200 mA/cm^2 was applied for 10 s, a process which resulted in the generation of self-standing nanoPS layers. Then, the samples were subjected to a thorough cleaning process in ethanol to eliminate any remaining. Table 1 presents the preparation conditions used to fabricate nanoPS membranes with different porosities.

Table 1
Summary of the preparation conditions of the self-standing nanoPS layers.

Sample name	Anodization current density (mA/cm^2)	Anodization time (second)	Layer thickness (μm)
PS10	10	3000	45
PS40	40	3000	87
PS60	60	3000	106

2.3. CHARACTERIZATION TECHNIQUES

The optical reflectance and transmittance spectra of the self-standing porous silicon layers were carried out in the 400 to 900 nm wavelength range using a Jasco V-560 double-beam spectrophotometer,

equipped with an integrating sphere to avoid scattering losses.

3. Experimental Results And Discussions

For the study of the optical properties of porous silicon, self-standing layers with different porosities were studied. The optical constants (n , index of refraction and k , extinction coefficient) were determined from the experimental reflectance and transmittance spectra shown in Figs. 1.a and 1.b, respectively.

The increase in the porosity of porous silicon layer leads to a reduction in the optical reflectance and an increase in the transmittance as shown in Fig. 1. This behavior is attributed to the change in the morphology and the chemical composition difference between bulk silicon and porous silicon. Porous silicon can be described as an homogeneous mixture of air, amorphous silicon, silicon nanocrystallites and silicon dioxide [10]. Accordingly, the increase in the porosity leads to increased optical transparency of the membranes as portrayed in Fig. 1.b. Furthermore, the extremely low optical transmission of porous silicon in the 400 to 550 nm range is attributed to the very large absorption of porous silicon in the UV-visible region of the electromagnetic spectrum.

From the modeled R and T spectra, the optical constants n and k were calculated for self-standing porous silicon layers of different porosity were determined using a simulation program based on the matrix method. Figures 2.a and 2.b show the spectral index of refraction and the spectral extinction coefficient as a function of wavelength of nanoPS self-standing layers with three different porosities. The reduction in the size of the Si nanocrystals which compose nanoPS with increasing etching current density leads to a reduction in the effective index of refraction and, at the same time, an increase in the extinction coefficient. This behavior is attributed to the different morphology and chemical composition of nanoPS layers grown under different fabrication parameters. This tendency is in agreement with the previously reported behavior of the optical constants of Al_2O_3 and GaN porous layers, where a reduction in the index of refraction was observed with increasing porosity [18, 19].

From the experimental results of the extinction coefficient, the absorption coefficient can be calculated with the relationship,

$$\alpha = \frac{4\pi k}{\lambda} (1)$$

Figure 3 portrays the relation between the absorption coefficient as a function of wavelength for nanoPS layers of different porosities. In all cases, the graphs show a reduction in α with increasing wavelength. In addition, α has higher values for low porosity samples (e.g. nanoPS 10 mA/cm²). This behavior is attributed to the reduction in the optical absorption at low porosity.

In addition, the values of the optical band gap for the nanoPS self-standing layers were extracted using Tauc plots [20]. Si is an indirect bandgap material in which the band gap energy equals 1.12 eV [21]. As has been previously demonstrated, the changes in the crystal structure and the morphology after etching

the Si wafers to fabricate nanoPS lead to widening the optical bandgap and to a direct bandgap character [22]. Accordingly, the relation between $(\alpha h\nu)^2$ and photon energy $(h\nu)$ was represented and is shown in Figs. 4.a, 4.b and 4.c for three self-standing layers with different porosities. The band gap energy value (E_g) can be calculated by extrapolating the straight line of the relation between $(\alpha h\nu)^2$ and $(h\nu)$. From the values of E_g it is concluded that an increase in the porosity of the nanoPS layers leads to an increase in the value of the optical E_g . This behavior is attributed to the change in the composition from bulk Si to a matrix of air (pores), amorphous silicon and Si nanocrystals [10, 15, 23]. Accordingly, the optical properties of nanostructured porous silicon can be adjusted depending on the intended application by the change in the morphology and porosity of the bulk material.

4. Conclusions

The values of the optical constants, n and k , and bandgap energy (E_g) of self-standing nanostructured porous silicon layers as a function of the fabrication parameters were determined using a simulation program based on the matrix method. The employed model in this work avoids the usual approximations. For instance, normal incidence angle for reflectance measurements, semi-infinite substrate, and homogeneous layers etc., as well as smoothness of the optical constants and the use of the criteria of continuity.

From the experimental results, it was found that increasing etching current density leads to a reduction in both the effective index of refraction and the extinction coefficient. However, from the experimentally determined values of E_g it is concluded that an increase in the porosity of the layers leads to an increase in the value of the optical bandgap, which is associated to a reduction in the size of the Si nanocrystals which compose nanoPS.

The accurate determination of the values of the optical constants of self-standing nanostructured porous silicon layers allows us to be specifically involve it in different photonic devices with the appropriate parameters and optimal performance.

Declarations

Acknowledgement

The authors are thankful to Mr. Luis García Pelayo and Dr. Valentin Constantin Nistor for technical support. This work was partially supported by Fundación de la Universidad Autónoma de Madrid (FUAM) and Minia University, Egypt.

AUTHOR DECLARATIONS

Funding: This research was partially funded by Universidad Autónoma de Madrid, FPI-UAM grant and by the Egyptian Ministry of Higher Education, Missions Section under Egyptian Joint Supervision Grant.

Conflict of Interest: The authors have no conflicts to disclose.

Author Contributions: **R. Ramadan:** Conceptualization (equal); formal analysis (equal); funding acquisition (equal); investigation (lead); methodology (lead); project administration (supporting); visualization (lead); writing – original draft (equal); writing – review and editing (equal). **R. J. Martín-Palma:** Conceptualization (equal); formal analysis (equal); funding acquisition (lead); Software (lead); project administration (lead); resources (lead); supervision (lead); visualization (supporting); writing – original draft (equal); writing – review and editing (equal).

Data availability: The data that support the findings of this study are available from the corresponding author upon reasonable request.

Consent for publication: Not applicable

References

1. Ramadan R, Abdel-Hady K, Manso-Silván M, Torres-Costa V (2019) Martín-Palma, Microwave plasma and rapid thermal processing of indium-tin oxide thin films for enhancing their performance as transparent electrodes. *J Photonics Energy* 9(3):034001
2. Reichelt K, Jiang X (1990) The preparation of thin films by physical vapour deposition methods. *Thin Solid Films* 191(1):91–126
3. Pentia E, Pintilie L, Matei I, Botila T, Pintilie I (2003) Combined chemical–physical methods for enhancing IR photoconductive properties of PbS thin films. *Infrared Phys Technol* 44(3):207–211
4. Kutavichus VP, Filippov VV, Huzouski VH (2006) Determination of optical parameters and thickness of weakly absorbing thin films from reflectance and transmittance spectra. *Appl Opt* 45(19):4547–4553
5. Vedam K, Knausenberger W, Lukes F (1969) Ellipsometric method for the determination of all the optical parameters of the system of an isotropic nonabsorbing film on an isotropic absorbing substrate. *Opt constants silicon JOSA* 59(1):64–71
6. Ramadan R, Torres-Costa V, Martín-Palma RJ (2021) Self-powered broadband hybrid organic–inorganic photodetectors based on PEDOT: PSS and silicon micro-nanostructures. *J Mater Chem C* 9(13):4682–4694
7. Ramadan R, Rodriguez C, Torres-Costa V, Pini V, Palma RJM, Cebrián V, Membibre RC, Ahumada O, Silván MM (2021) Bringing immuno-assemblies to optoelectronics: sandwich assay integration of a nanostructured porous-silicon/gold-nanoparticle phototransistor. *Mater Sci Engineering: B* 271:115271
8. Ramadan R, Manso-Silván M, Martín-Palma RJ (2020) Hybrid porous silicon/silver nanostructures for the development of enhanced photovoltaic devices. *J Mater Sci* 55(13):5458–5470
9. Canham L (2018) Routes of formation for porous silicon, *Handbook of Porous Silicon*, 2nd ed.; Springer: Berlin/Heidelberg, Germany 1 3–11

10. Ramadan R, Martín-Palma RJ (2020) Effect of electrolyte pH value and current density on the electrodeposition of silver nanoparticles into porous silicon. *J Nanophotonics* 14(4):040501
11. Torres-Costa V, Martín-Palma R (2010) Application of nanostructured porous silicon in the field of optics. A review. *J Mater Sci* 45(11):2823–2838
12. Naderi N, Hashim M (2012) A combination of electroless and electrochemical etching methods for enhancing the uniformity of porous silicon substrate for light detection application. *Appl Surf Sci* 258(17):6436–6440
13. Ohmukai M, Okada K, Tsutsumi Y (2005) Patterned porous silicon formed with photolithography. *J Mater Sci: Mater Electron* 16(2):119–121
14. Martín-Palma RJ, Martinez-Duart J, Macleod A (2000) Determination of the optical constants of a semiconductor thin film employing the matrix method. *IEEE Trans Educ* 43(1):63–68
15. Martín-Palma RJ, McAtee PD, Ramadan R, Lakhtakia A (2019) Hybrid nanostructured porous silicon-silver layers for wideband optical absorption. *Sci Rep* 9(1):1–8
16. Palik ED (1998) *Handbook of optical constants of solids*, Academic press
17. Bueno R, Trigo J, Martínez-Duart J, Elizalde E, Sanz J, Vacuum A (1995) *Surfaces, and Films* 13(5) 2378–2383
18. Berman D, Guha S, Lee B, Elam JW, Darling SB, Shevchenko EV (2017) Sequential infiltration synthesis for the design of low refractive index surface coatings with controllable thickness. *ACS Nano* 11(3):2521–2530
19. Alquran MK, Bejugam V Assessment of the Enhancement for the Excitation Emission in Porous GaN Using Photoluminescence
20. Tauc J, Grigorovici R, Vancu A (1966) Optical properties and electronic structure of amorphous germanium. *Phys status solidi (b)* 15(2):627–637
21. Collings PJ (1980) Simple measurement of the band gap in silicon and germanium. *Am J Phys* 48(3):197–199
22. Mortezaali A, Sani SR, Jooni FJ (2009) Correlation between porosity of porous silicon and optoelectronic properties. *J Non-Oxide Glasses* 1:293–299
23. Dzhafarov T, Yuksel SA (2011) Nano-porous silicon-based mini hydrogen fuel cells, book: *Alternative Fuel*.—Rijeka: Intech309–346

Figures

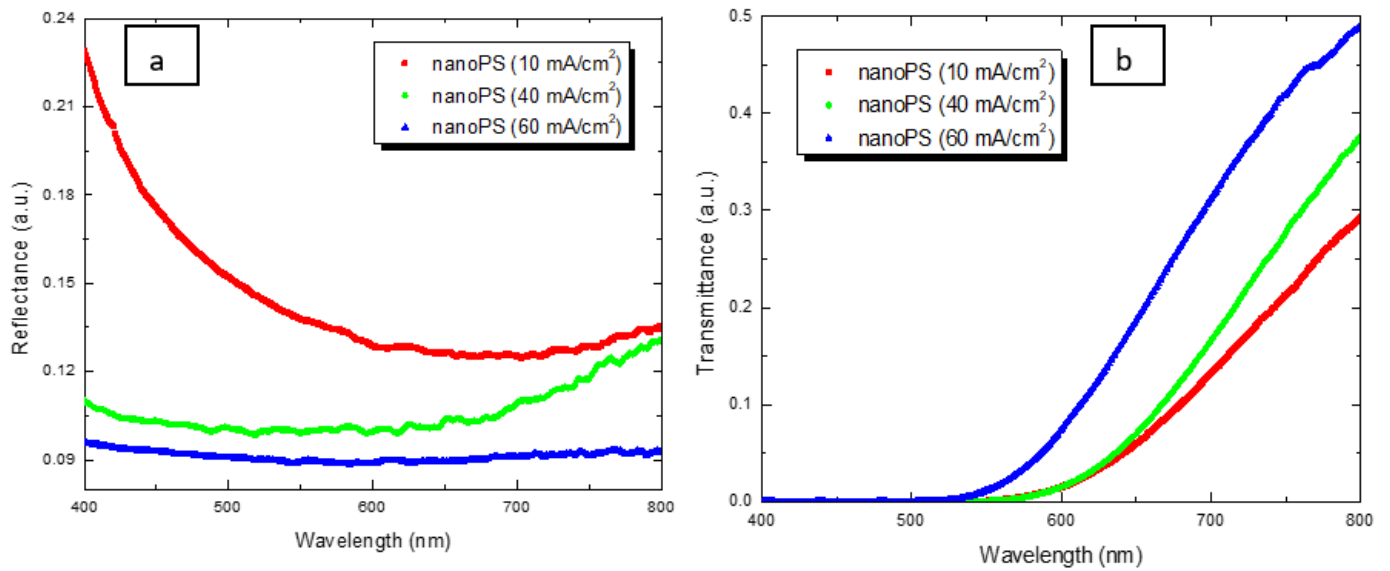


Figure 1

Experimental (a) reflectance and (b) transmittance spectra in the visible wavelength range of nanostructured porous silicon layers with different porosities (different etching current densities).

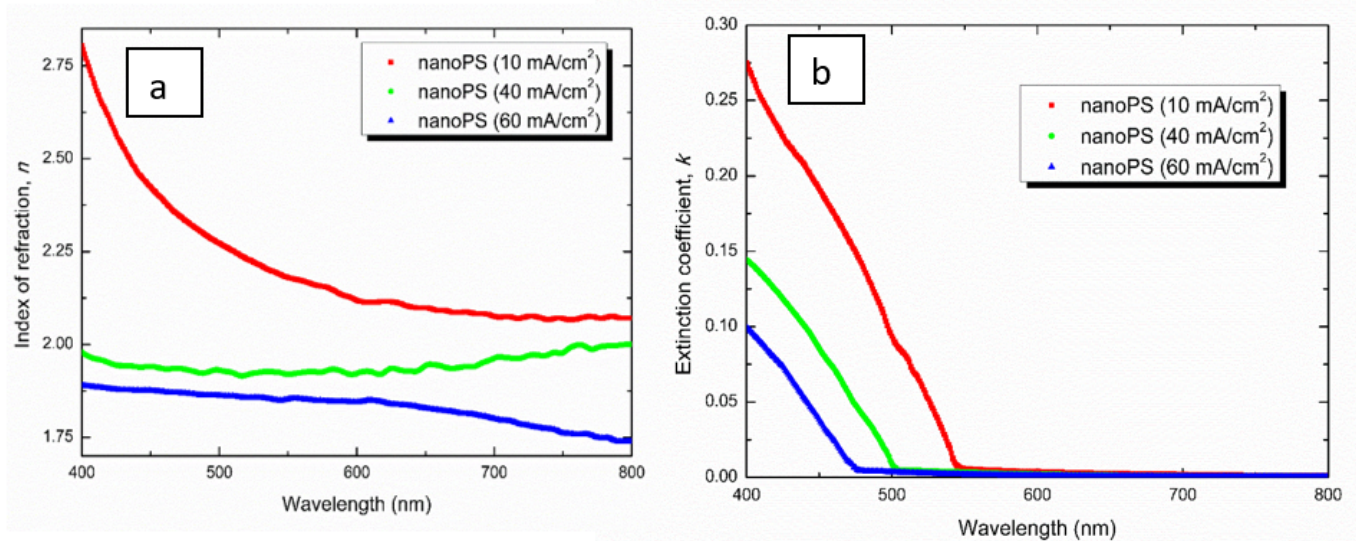


Figure 2

Optical properties of self-standing nanoPS layers with different porosities in the 400 nm to 800 nm wavelength range. (a) Index of refraction. (b) Extinction coefficient.

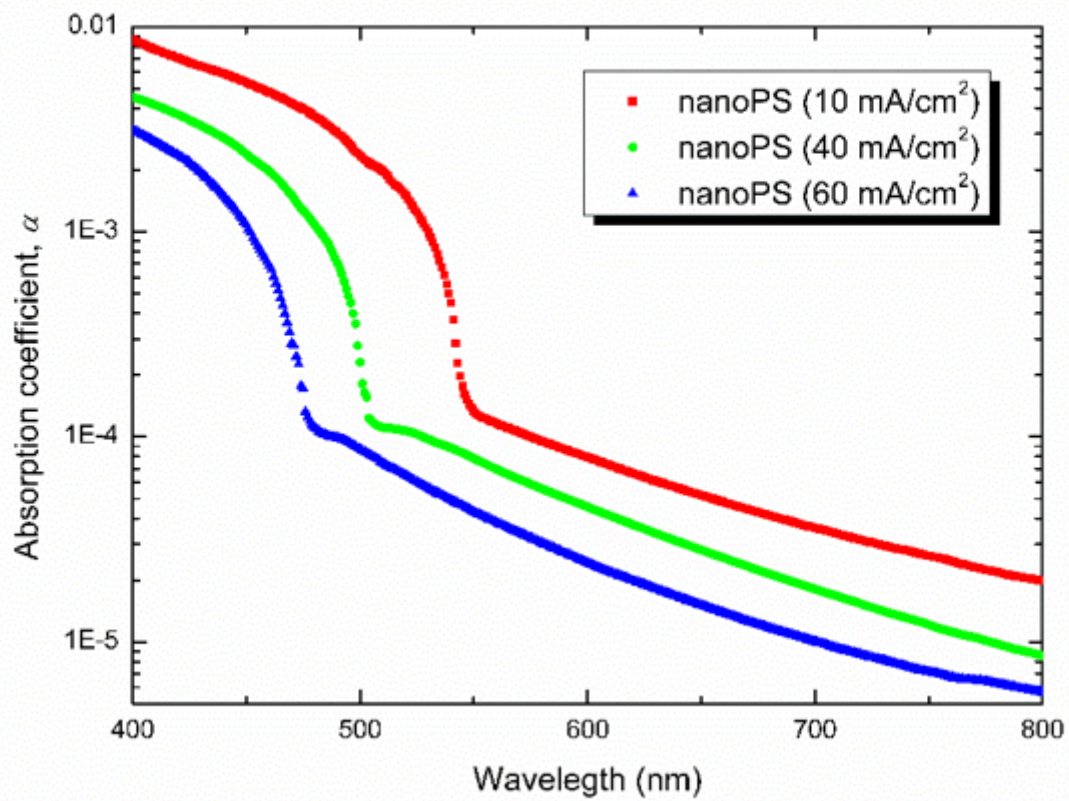


Figure 3

Absorption coefficient (α) as a function of wavelength for three nanoPS layers with different porosities.

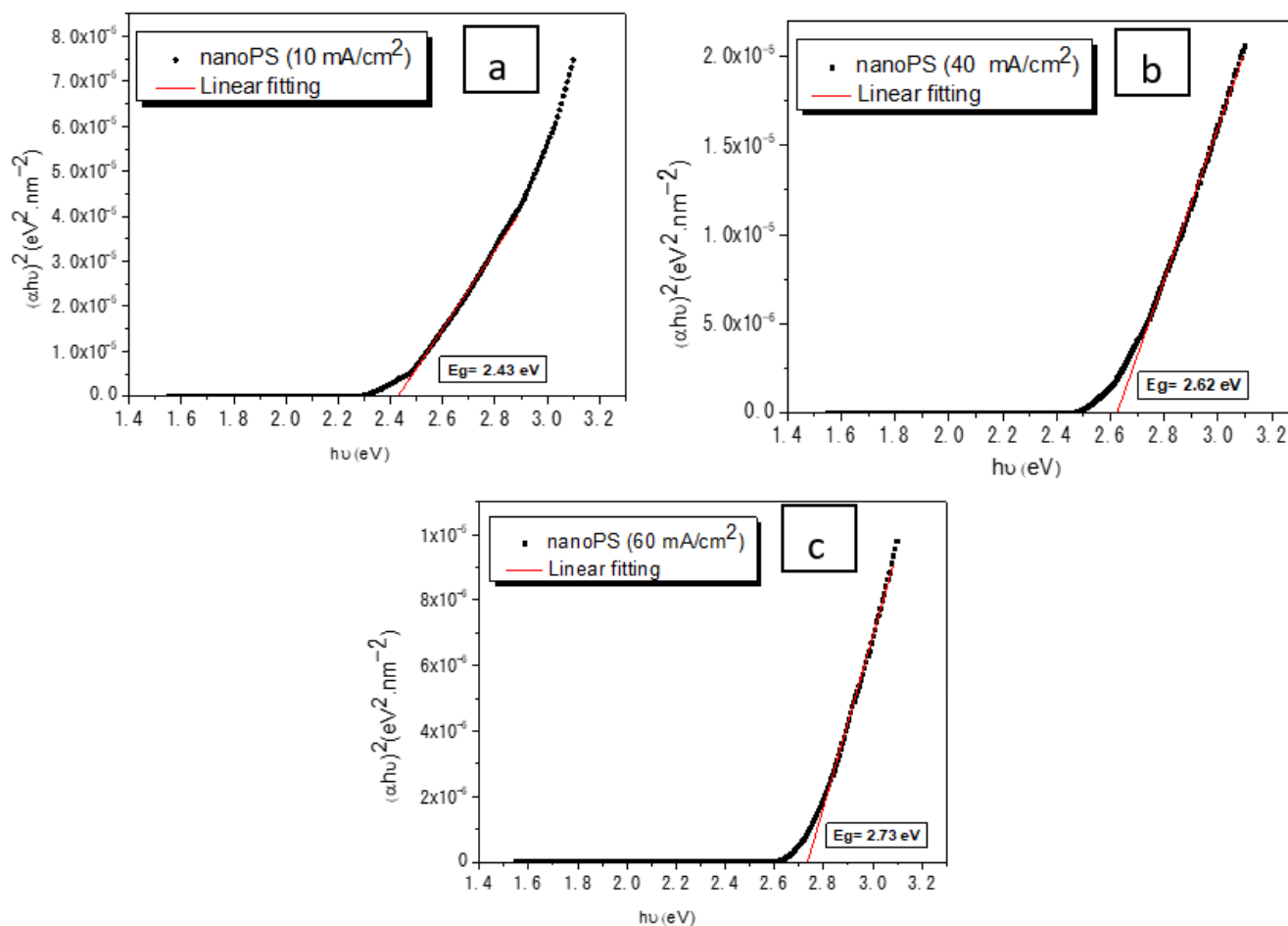


Figure 4

Tauc plots showing the direct bandgap character of the fabricated nanoPS layers. a) nanoPS layer fabricated at 10 mA/cm² current density, b) nanoPS layer fabricated at 40 mA/cm² current density and c) nanoPS layer fabricated at 60 mA/cm² current density.